Nanosatellite Three-Axis Attitude Control and Determination Using Two Magnetorquers Only

Danil Ivanov
Space System Dynamics Department
Keldysh Institute of Applied Mathematics RAS
Moscow, Russia
ORCID: 0000-0002-8253-7092

Dmitry Roldugin
Space System Dynamics Department
Keldysh Institute of Applied Mathematics RAS
Moscow, Russia
ORCID: 0000-0002-9616-0994

***Abstract* — The paper considers two magnetorquers as the sole attitude control system unit used both for control and determination. An algorithm of the three-axis attitude determination is proposed. It utilizes the measurements of the electromotive force induced in magnetorquers during the free motion of the satellite when the control is not applied. The extended Kalman filter is used. The estimation of the state vector consisting of the vector part of quaternion and the angular velocity vector is used for the control calculation. Three axis attitude is achieved with the same magnetorquers using the Lyapunov control approach. The paper studies the accuracy of the developed algorithm, its dependence on orbit inclination and orbit altitude.**

Keywords — attitude control, attitude determination, magnetorquers, CubeSat

I. INTRODUCTION

Active magnetic attitude control system is the most common for micro- and nanosatellites in LEO. It is used for the angular velocity damping, stabilization along the geomagnetic induction vector, spin stabilization and even three-axis attitude acquisition. Proper stabilization requires the real-time determination of the attitude motion. It is obtained by processing the attitude sensors measurements. Sun sensors [1], [2], magnetometers [3]–[5], angular velocity sensors [6], [7] and even micro star tracker [8], [9] are commonly used for the attitude motion determination. However, tendency for the miniaturization and simplification leads to the control system with the minimal set of hardware. For example, the three axis attitude control is available with magnetometer and three magnetorquers for a CubeSat [10], [11]. Note that COTS sensors are prone to faults and small satellites rarely benefit from any backup measures. So there is a high risk of early mission loss because of the magnetometer failure. However, it is still possible to determine the angular motion using measurements of the induced electromotive force (EMF) in magnetorquers.

This paper considers the satellite equipped with the solenoid magnetorquers, i.e. coils wound into a tightly packed helix. The magnetic flux enclosed by the non-operating coil is changing due to the angular motion in the geomagnetic field. According to the well-known Faraday's law, this causes the induced EMF in magnetorquers. It may be measured by the analog-to-digital converter and then processed by the extended Kalman filter. The attitude information is available during the uncontrolled motion of the satellite. Afterwards the necessary control torque may be implemented using the same magnetorquers.

The paper is a continuation of the authors previous work [12], where the attitude determination and control is considered using three magnetorquers. In the current work the failure of one of the magnetorquers is considered. An extremely limited hardware set is used to achieve the three-axis stabilization. This paper studies the accuracy of the proposed control scheme and its dependence on the orbit inclination and orbit altitude.

II. ATTITUDE MOTION EQUATIONS

Rigid spacecraft angular motion is considered. The satellite is equipped with three mutually orthogonal magnetorquers. Two reference frames are used:

$OX_1X_2X_3$ is the orbital reference frame located at the satellite center of mass. OX_3 is directed along the satellite radius-vector, OX_1 is directed along the orbital velocity, OX_2 is directed so that the reference frame is right-handed;

$Ox_1x_2x_3$ is the body reference frame, its axes coincide with the principal axes of inertia of the satellite.

Satellite attitude is represented using Euler angles α, β, γ (rotation sequence 1-2-3); direction cosines matrix $\mathbf{A}$ and its elements a_{ij}; and quaternion $\Lambda = (\mathbf{q}, q_0)$. Angular velocity may represent either the absolute motion ($\boldsymbol{\omega}$ and its components ω_i) or relative motion with respect to the orbital reference frame ($\boldsymbol{\Omega}$ and Ω_i). The absolute and relative velocities are related by

$$\boldsymbol{\omega} = \boldsymbol{\Omega} + \mathbf{A}\boldsymbol{\omega}_{orb},$$

where $\boldsymbol{\omega}_{orb} = (0,\ \omega_0,\ 0)$ is the orbital reference frame angular velocity. Euler equations for the satellite with inertia tensor $\mathbf{J} = \mathrm{diag}(A, B, C)$ are

$$\mathbf{J}\dot{\boldsymbol{\omega}} + \boldsymbol{\omega} \times \mathbf{J}\boldsymbol{\omega} = \mathbf{M}.$$

The torque $\mathbf{M}$ may contain the control part $\mathbf{M}_{ctrl}$ and the disturbing part. The latter is divided into the gravitational $\mathbf{M}_{gr}$ and the unknown one $\mathbf{M}_{dist}$ so overall $\mathbf{M} = \mathbf{M}_{ctrl} + \mathbf{M}_{gr} + \mathbf{M}_{dist}$. The control torque is

$$\mathbf{M}_{ctrl} = \mathbf{m} \times \mathbf{B},$$

where $\mathbf{m}$ is the dipole control moment of the satellite, $\mathbf{B}$ is the geomagnetic induction vector in the bound reference frame. Gravitational torque is

$$\mathbf{M}_{gr} = 3\omega_0^2 (\mathbf{A}\mathbf{e}_3) \times \mathbf{J}(\mathbf{A}\mathbf{e}_3),$$

where $\mathbf{e}_3 = (0, 0, 1)$ is the satellite radius-vector in the orbital frame. Disturbing torque $\mathbf{M}_{dist}$ is modeled as a random noise with the Gaussian distribution of the order of 5·10-8 N·m.

The dynamical equation for the relative motion is

$$\mathbf{J}\dot{\mathbf{\Omega}} = \mathbf{M} + \mathbf{M}_{gir} + \mathbf{J}\mathbf{\Omega} \times \mathbf{A}\boldsymbol{\omega}_{orb}, \quad (1)$$

where $\mathbf{M}_{gir} = -\boldsymbol{\omega} \times \mathbf{J}\boldsymbol{\omega}$ is the gyroscopic torque.

Dynamical equations are supplemented with the kinematic relations. Quaternion kinematics is

$$\begin{aligned} \dot{\mathbf{q}} &= \frac{1}{2}\left(q_0 \mathbf{\Omega} + \mathbf{W}_{\Omega}\mathbf{q}\right), \\ \dot{q}_0 &= -\frac{1}{2}\mathbf{q}^T \mathbf{\Omega}, \end{aligned} \quad (2)$$

where $\mathbf{W}_{\mathbf{y}}$ is a skew-symmetric matrix for any vector $\mathbf{y}$,

$$\mathbf{W}_{\mathbf{y}} = \begin{pmatrix} 0 & y_3 & -y_2 \\ -y_3 & 0 & y_1 \\ y_2 & -y_1 & 0 \end{pmatrix}.$$

The inclined dipole model is mainly used to represent the geomagnetic field [13]. It allows quite accurate field representation [14] paired with simple computational procedures. The geomagnetic induction vector is

$$\mathbf{B} = \frac{\mu_e}{r^5}\left(\mathbf{k}r^2 - 3(\mathbf{k}\mathbf{r})\mathbf{r}\right),$$

where $\mathbf{k}$ is the Earth's dipole unit vector and $\mathbf{r}$ is the satellite radius-vector, r is the satellite radius vector magnitude, $\mu_e = 7.812 \cdot 10^6$ km3·kg·s-2·A-1. The direct dipole model ($\mathbf{k}$ is antiparallel to the Earth rotation axis) is used for analytical approaches, the geomagnetic induction vector in the orbital frame in this model is

$$\mathbf{B}_{orb} = B_0 \begin{pmatrix} \cos u \sin i \\ \cos i \\ -2 \sin u \sin i \end{pmatrix}, \quad (3)$$

where $B_0 = \mu_e / r^3$, u is the argument of latitude, i is the orbit inclination.

III. Magnetorquers Measurement Model

Magnetic coils, also referred to as magnetorquers, are especially valuable for CubeSat-class nanosatellites. They are commercially available in two typical configurations: in loose coils of flat wound wire and in tightly wound coils around a permalloy rod. Both magnetorquers configurations are often combined in one ready-to-use board. Such a board is used, for example, in Delfi-n3Xt CubeSat [15] (see Fig.1). It consists of a set of two x and y axis magnetorquer rods and one z axis air core magnetorquer.

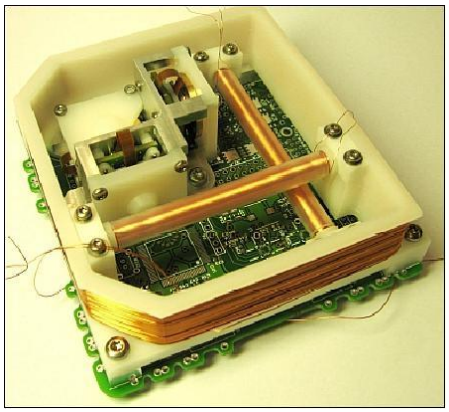

Fig. 1. Magnetorquers of Delfi-n3Xt [15]

Consider the CubeSat with two orthogonal magnetorquer coils. In case of the passive attitude motion the magnetorquers do not produce any commanded control moment. Since the satellite rotates in the geomagnetic field, an EMF V is induced in the coil according to the Faraday's law:

$$V_i = -N\frac{d\Phi_i}{dt} = -NS\frac{d(\mathbf{B}, \mathbf{n}_i)}{dt}, \; i = 1, 2, \quad (4)$$

where Φ is the magnetic flux passing through the coil with the area S and with a number of turns N, $\mathbf{n}_i$ are normal vectors to the coils planes. Assume that vectors $\mathbf{n}_i$ are directed along the satellite reference frame axes. Then Eq. (4) can be rewritten as:

$$\mathbf{V} = -NS\frac{d\mathbf{B}}{dt}.$$

In case of the magnetorquer rods it is necessary to take into account the auxiliary magnetic field $\mathbf{H}$ inside the rod material. It is related to the geomagnetic field $\mathbf{B}$ as

$$\mathbf{B} = \mu\mathbf{H},$$

where μ is the core permeability. Ferromagnetic core strengthens the external magnetic field in the coil and increases the output signal:

$$\mathbf{V} = -NS\mu\frac{d\mathbf{H}}{dt}.$$

That is why despite of the small coil area of the magnetorquer rod compared to the air core coil, its EMF may be larger due to the large value of μ (about $10^5 \mu_0$, μ_0 is the magnetic constant). However, the relative permeability of the core μ_c may be much lower than the material permeability [16].

To use the EMF measurements in the attitude determination process it is necessary to convert the analog signal V into the digital value. The most critical feature of the analog-to-digital converter (ADC) is its sensitivity. If the reference signal of the ADC is 1 V then the 16-bit converter has the resolution of about 15 μV [17]. This is the minimum value that can be theoretically detected. However, the ADC are subjected to errors due to the thermal noise in electrical circuit, errors in temperature bias etc. At best the errors do not exceed 2 bits signal values. That is why digital measures are noisy, and the final measurement model is:

$$\mathbf{V} = -NS\frac{d\mathbf{B}}{dt} + \boldsymbol{\eta}_V, \tag{5}$$

where $\boldsymbol{\eta}_V$ is the noise that is considered to be normally distributed.

Note that according to the model (5) the residual magnetic dipole moment of the satellite does not affect the measurements in the case it is constant. So, the problem of taking into account constant satellite self magnetic field does not exist in the case of electromotive force measurements contrary to utilizing magnetometer measurements. However, there may be changing satellite magnetic filed caused by currents in the onboard devices on satellite which will increase the measurement errors.

IV. Extended Kalman Filter Application

A. Kalman Filter Basics

The Extended Kalman Filter (EKF) is a well-known and well-established algorithm. It is characterized by the relatively small computational cost and provides the estimation of the state vector that is not directly measured.

Kalman filter is a recursive algorithm that uses the dynamical system model and sensor readings for the actual motion determination. The state vector estimation $\hat{\mathbf{x}}_{k-1}^{+} = \hat{\mathbf{x}}(t_k)$ is calculated for each discrete time step t_k when the measurements are available. The discrete Kalman filter utilizes the correction of the previous estimate [18]. Consider step $k-1$ along with the corresponding state vector estimation $\hat{\mathbf{x}}_{k-1}^{+}$ and covariance matrix $\mathbf{P}_{k-1}^{+}$. The goal is to find the state vector estimation for the next step $\hat{\mathbf{x}}_k^{+}$. First the a priory estimate $\hat{\mathbf{x}}_k^{-}$ is formed using straight mathematical model integration. It is corrected using the sensor measurements vector $\mathbf{z}_k$ to obtain the a posteriori estimate $\hat{\mathbf{x}}_k^{+}$. The covariance error matrix $\mathbf{P}_k^{-}$ is also constructed from the previous step information using Riccati equation. It is then updated to $\mathbf{P}_k^{+}$ using measurements.

Kalman filter is designed for linear mathematical models and allows the best mean-square state vector estimation. However, it may be extended for any non-linear mathematical models of both the dynamical system and the measurements,

$$\dot{\mathbf{x}}(t) = \mathbf{f}(\mathbf{x}, t) + \mathbf{G}\mathbf{w}(t),$$
$$\dot{\mathbf{z}}(t) = \mathbf{h}(\mathbf{x}, t) + \mathbf{v}(t),$$

where $\mathbf{w}(t)$ is the Gaussian dynamical model error with the covariance matrix $\mathbf{D}$, $\mathbf{G}$ is the matrix of influence of the model error on the state vector, $\mathbf{v}(t)$ is the Gaussian measurements error with the covariance matrix $\mathbf{R}$.

EKF requires the decomposition of the right-side functions $\mathbf{f}(\mathbf{x}, t)$ and $\mathbf{h}(\mathbf{x}, t)$ into the Taylor series in the vicinity of the current state vector. Only linear terms are used in the filter. The dynamical system matrix $\mathbf{F}$ and measurements model $\mathbf{H}$ matrix are

$$\mathbf{F}_k = \left.\frac{\partial \mathbf{f}(\mathbf{x}, t)}{\partial \mathbf{x}}\right|_{\mathbf{x}=\hat{\mathbf{x}}_k^{-}, t=t_k}, \quad \mathbf{H}_k = \left.\frac{\partial \mathbf{h}(\mathbf{x}, t)}{\partial \mathbf{x}}\right|_{\mathbf{x}=\hat{\mathbf{x}}_k^{-}, t=t_k}.$$

The discrete EKF uses the non-linear dynamical and measurements models for a priory estimate prediction and a posteriori correction [19]. The prediction phase is

$$\hat{\mathbf{x}}_k^{-} = \int_{t_{k-1}}^{t_k} \mathbf{f}(\mathbf{x}, t)dt,$$
$$\mathbf{P}_k^{-} = \boldsymbol{\Phi}_k \mathbf{P}_{k-1}^{+} \boldsymbol{\Phi}_k^{\mathrm{T}} + \mathbf{Q}_k,$$

where $\mathbf{Q}_k$ is the covariance matrix of the discrete-time process noise, it is calculated as

$$\mathbf{Q}_k = \int_{t_{k-1}}^{t_k} \boldsymbol{\Phi}_k \mathbf{G}\mathbf{D}\mathbf{G}^T \boldsymbol{\Phi}_k^T dt. \tag{6}$$

The correction phase is

$$\mathbf{K}_k = \mathbf{P}_k^{-}\mathbf{H}_k^{\mathrm{T}}\left(\mathbf{H}_k\mathbf{P}_k^{-}\mathbf{H}_k^{\mathrm{T}} + \mathbf{R}_k\right)^{-1},$$
$$\hat{\mathbf{x}}_k^{+} = \hat{\mathbf{x}}_k^{-} + \mathbf{K}_k\left(\mathbf{z}_k - \mathbf{h}\left(\hat{\mathbf{x}}_k^{-}, t_k\right)\right),$$
$$\mathbf{P}_k^{+} = \left(\mathbf{E} - \mathbf{K}_k\mathbf{H}_k\right)\mathbf{P}_k^{-},$$

where $\boldsymbol{\Phi}_k = \exp\left(\mathbf{F}_k\left(t_k - t_{k-1}\right)\right)$ is the transition matrix between the states $k-1$ and k, $\mathbf{E}$ is an identity matrix, $\mathbf{K}$ is the weighing matrix.

B. Linearized Equations

The EKF to obtain the satellite attitude in the orbital reference frame should be constructed. The state vector is

$$\mathbf{x} = (\mathbf{q}, \boldsymbol{\Omega}).$$

Dynamical model of the controlled satellite angular motion is presented by Eq. (1), quaternion kinematic equation as in Eq.(2) is used. Equations of motion should be

linearized in the vicinity of the current state vector. Rewrite Eqs. (1), (2) as

$$\delta\dot{\mathbf{x}}(t) = \mathbf{F}(t)\,\delta\mathbf{x}(t),$$

where $\delta\mathbf{x}(t)$ is a small state vector increment, $\mathbf{F}(t)$ is the matrix of the equations of motion linearized in the vicinity of the current state. After linearization the obtained dynamics matrix $\mathbf{F}$ is as follows

$$\mathbf{F} = \begin{pmatrix} -\mathbf{W}_{\boldsymbol{\Omega}} & \frac{1}{2}\mathbf{E} \\ \mathbf{J}^{-1}\mathbf{F}_{qw} & \mathbf{J}^{-1}\left(\mathbf{F}_{gir}^{\boldsymbol{\Omega}} - \mathbf{W}_{\mathbf{A}\boldsymbol{\omega}_{orb}}\mathbf{J}\right) \end{pmatrix},$$

where

$$\mathbf{F}_{qw} = 6\omega_0^2\mathbf{F}_{gr} + \mathbf{F}_{gir}^{\mathbf{q}} + 2\mathbf{W}_{\mathbf{J}\boldsymbol{\Omega}}\mathbf{W}_{\mathbf{A}\boldsymbol{\omega}_{orb}} + 2\mathbf{W}_{\mathbf{m}}\mathbf{W}_{\hat{\mathbf{B}}},$$
$$\mathbf{F}_{gr} = \mathbf{W}_{\mathbf{Ae}_3}\mathbf{J}\mathbf{W}_{\mathbf{Ae}_3} - \mathbf{W}_{\mathbf{JAe}_3}\mathbf{W}_{\mathbf{Ae}_3},$$
$$\mathbf{F}_{gir}^{\boldsymbol{\Omega}} = \mathbf{W}_{\mathbf{J}\boldsymbol{\Omega}} - \mathbf{W}_{\boldsymbol{\Omega}}\mathbf{J},$$
$$\mathbf{F}_{gir}^{\mathbf{q}} = 2\left(\mathbf{W}_{\mathbf{J}\boldsymbol{\omega}}\mathbf{W}_{\mathbf{A}\boldsymbol{\omega}_{orb}} - \mathbf{W}_{\boldsymbol{\omega}}\mathbf{J}\mathbf{W}_{\mathbf{A}\boldsymbol{\omega}_{orb}}\right).$$

Using the relation $\mathbf{B} = \mathbf{A}\mathbf{B}_{orb}$ the magnetorquer measurements model Eq. (5) can be rewritten as:

$$\mathbf{z} = -NS\frac{d\left(\mathbf{A}\mathbf{B}_{orb}\right)}{dt} + \boldsymbol{\eta}_V = -NS\left[-\boldsymbol{\Omega}\times\mathbf{B} + \mathbf{A}\left(\boldsymbol{\omega}_0\times\mathbf{B}_{orb}\right)\right] + \boldsymbol{\eta}_V,$$

where $\boldsymbol{\eta}_V$ is a Gaussian geomagnetic induction vector error with zero mean. The measurements matrix after the linearization is as follows

$$\mathbf{H} = -NS\left[-2\mathbf{W}_{\boldsymbol{\Omega}}\mathbf{W}_{\hat{\mathbf{B}}} - 2\mathbf{W}_{\mathbf{A}\mathbf{B}_{orb}} \quad \mathbf{W}_{\hat{\mathbf{B}}}\right].$$

The expression for measurement matrix is obtained for three magnetorquers [12]. Since in the paper only two magnetorquers are considered, then the dimension of the measurement vector $\mathbf{z}$ is 2. In this case the measurement matrix $\mathbf{H}$ has just two rows from the expression above.

The proposed attitude determination approach is supplemented with the attitude control algorithm.

V. Magnetic Control Algorithm

Consider the Lyapunov-based control

$$\mathbf{m} = -k_{\omega}\mathbf{B}\times\boldsymbol{\Omega} - k_a\mathbf{B}\times\mathbf{S}, \qquad (7)$$

where $\mathbf{S} = \left(a_{23} - a_{32},\ a_{31} - a_{13},\ a_{12} - a_{21}\right)$, k_a, k_{ω} are the control parameters. This is the common approach when magnetorquers implement the Lyapunov control part that is perpendicular to the geomagnetic induction vector. This control ensures the necessary attitude [20]–[22] provided that the control parameters are small enough and carefully adjusted. The adjustment is conducted in two steps. First the equations of motion are linearized in the vicinity of the necessary attitude. These equations utilize the direct dipole geomagnetic field. They do not take into account any disturbances other than the gravity.

Linearized equations introduce the derivative with respect to the argument of latitude. These equations are analyzed using the Floquet theory [23]. Fig. 1 represents the characteristic multipliers in the vicinity of the stability area of the linearized equations of motion.

The satellite and its orbit parameters are as follows:

- circular orbit, altitude 400 km, inclination 51.7°, Earth radius 6371 km;

- inertia tensor $\mathbf{J} = \mathrm{diag}\left(5\cdot10^{-3},\ 6\cdot10^{-3},\ 7\cdot10^{-3}\right)$ kg·m2.

Control parameters can be found from Fig. 2 only approximately. So the second adjustment step is necessary. Initial equations of motion (with some additional disturbances, more complex geomagnetic field model etc.) are modeled numerically with the control parameters close to the theoretically optimal ones. For the considered case good control parameters are $k_{\omega} = 40/\omega_0$, $k_a = 12$ N·m/T2. Note that they are very close to the optimal ones according to Fig. 2.

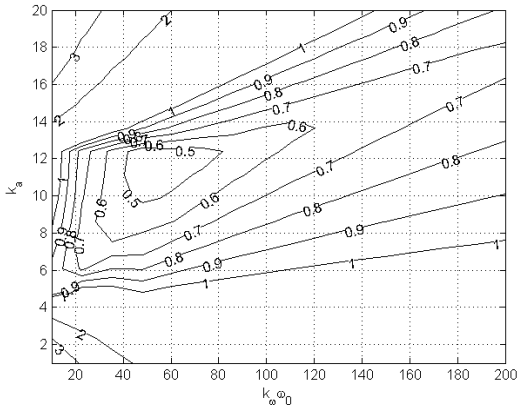

Fig. 2. Stability area

In the case of two magnetorquers the full magnetic vector $\mathbf{m}$ calculated from (7) cannot be implemented. Nevertheless the two of the three components are still tending the attitude to the orbital one, however, the accuracy of stabilization is worsened. To study the achievable attitude stabilization and attitude estimation accuracy the numerical study is performed.

VI. Numerical Study

Consider the 1U CubeSat with the orbit and mass parameters provided above. It is equipped with two orthogonal magnetorquers with the rod diameter $d = 5.7$ mm, so the area is $S = 10^{-4}$ m2, the rod relative permeability is 75000 and the number of turns is $N = 6000$ each (these parameters are similar to the magnetorquer described in [24]). The magnetorquers are placed along the x and y axis in the body reference frame.

Filter initialization requires definition of the measurements errors matrix $\mathbf{R}$, motion equations model

errors matrix $\mathbf{Q}$ and initial estimation errors of the state vector matrix $\mathbf{P}_0$.

Consider the standard measurements deviation of the induced EMF to be σ_{meas}=50 μV. Then the measurements errors covariance matrix is assumed to be $\mathbf{R} = diag\left(\sigma_{meas}^2, \sigma_{meas}^2\right)$.

The unaccounted disturbing torque is supposed to be random and of the order of $d = 5 \cdot 10^{-8}$ N·m, its distribution is Gaussian with zero mean. The model error covariance matrix is calculated using Eq. (6). Integration of the Eq. (6) is rather complicated, especially for the nanosatellite on-board computer. It is reasonable to simplify this expression using the reduced and constant state transition matrix as:

$$\mathbf{\Phi} = \begin{bmatrix} \mathbf{E} & \frac{1}{2}\mathbf{E}\Delta t \\ 0_{3x3} & \mathbf{E} \end{bmatrix}.$$

The matrix of the influence of the model error on the state vector is determined as

$$\mathbf{G} = \begin{bmatrix} 0_{3x3} \\ \mathbf{J}^{-1} \end{bmatrix}.$$

Then, the model errors covariance matrix is derived from Eq. (6) as follows

$$\mathbf{Q} = \begin{bmatrix} \mathbf{E}\sigma_q^2 & \mathbf{E}\sigma_\omega\sigma_q \\ \mathbf{E}\sigma_\omega\sigma_q & \mathbf{E}\sigma_\omega^2 \end{bmatrix}, \ \sigma_\omega = I^{-1} d\Delta t, \ \sigma_q = I^{-1} d\Delta t^2 / 2,$$

where I is the smallest inertia moment, Δt is the measurements sampling interval, d is the mean square deviation of the disturbance torque acting on the satellite.

The initial state vector estimation is arbitrary. Suppose it to be zero (zero vector part of quaternion and zero angular velocity). Consider the maximum quaternion error $\sigma_{q_0} = 1$ and knowingly big velocity error $\sigma_{\omega_0} = 10$ deg/s. The initial error matrix is

$$\mathbf{P}_0 = diag\left(\sigma_{q_0}^2, \sigma_{q_0}^2, \sigma_{q_0}^2, \sigma_{\omega_0}^2, \sigma_{\omega_0}^2, \sigma_{\omega_0}^2\right),$$

Set the initial angular velocity $\boldsymbol{\omega}(t=0) = \left(10\omega_0, 10\omega_0, 10\omega_0\right)$, where the orbital angular velocity $\omega_0 = 0.06$ deg/s, and initial quaternion $\Lambda_0 = \left[1\ 0\ 0\ 0\right]$. The sampling measurements time is 1 s.

Consider the application of the proposed attitude determination and control algorithms with two magnetorquers for the three-axis stabilization. The following simulation results are obtained for the ISS orbit. Fig. 3 shows the direction cosines between the body and orbital reference frames and relative angular velocity. The satellite is stabilized in the orbital reference frame with the accuracy of about 20 deg in 5 hours. Comparing to the case of three magnetorquers with the same parameters (see [12]) the attitude error is doubled. Nevertheless, at least coarse stabilization is achieved.

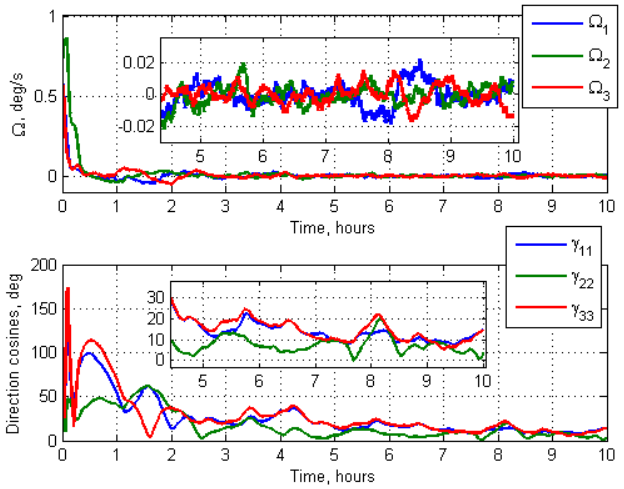

Fig. 3. Angular velocity and direction cosines angles during control motion

Fig. 4 shows the induced EMF in the two magnetorquers. One can see that the measurements are quite noisy, but the signal-to-noise ratio after the stabilization is close to 5. Fig. 5 presents the EKF state vector estimation errors. The estimations finally converged after about 3 hours and the accuracy is less than 8 deg. The difference between the estimated and obtained EMF measurements are shown in Fig. 6. After the convergence the residuals are close to the normal distributed random value with defined in the simulation σ_{meas}=50 μV. The EKF estimations are close to the adequate values.

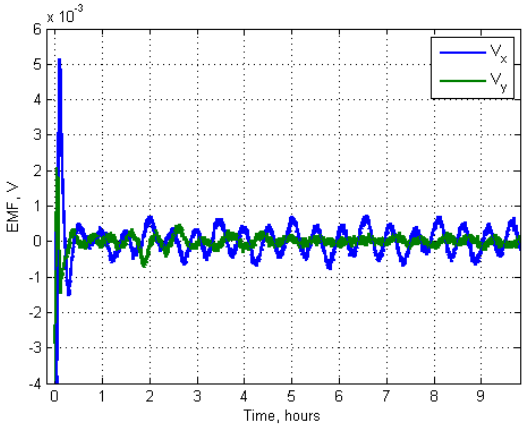

Fig. 4. Measurements of the induced EMF in the magnetorquers

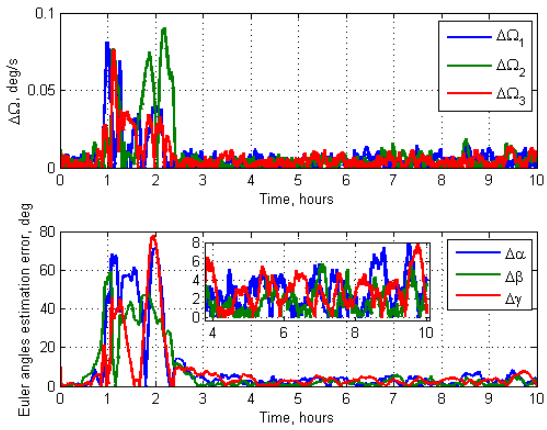

Fig. 5. Accuracy of the attitude motion estimation

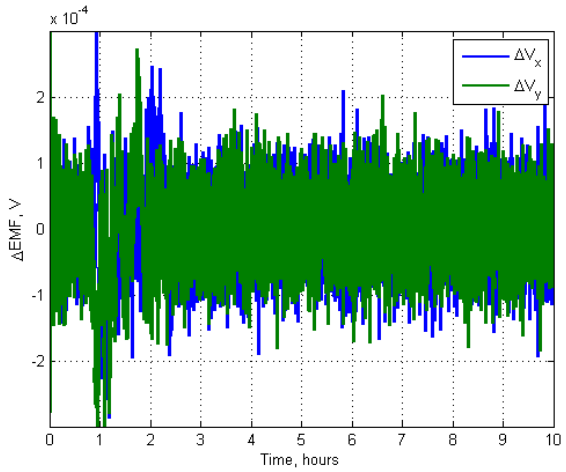

Fig. 6. Residuals of the measurements

Covariance matrix of the state vector may be used to calculate the expected errors of the state vector estimations by EKF. Fig. 7 shows the 3σ expected values calculated using the diagonal elements of matrix $\mathbf{P}$. The actual errors are in the predicted area. The error for the second angle β is less than for α and γ because of the absence of one of the magnetorquers. It is also should be noted that the estimation accuracy is also about 2 times worse than in the case of three magnetorquers.

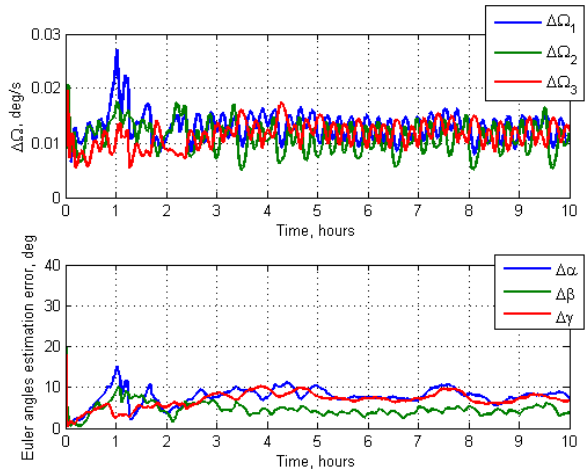

Fig. 7. Accuracy of the attitude motion estimation calculated using the covariance matrix

Consider the dependence of the stabilization and estimation accuracy on the orbit inclination. The results are stochastic due to the random measurement errors and disturbances included in the simulation. A set of numerical experiments is carried out with the same parameters except for the inclination. The results are expressed in the box plots. Half of the results are inside the box, the dot indicates the mean value, and one quarter of the results lie below and above the box. Crosses indicate the values outside of 3σ (assuming that the data is normally distributed). Fig. 8 and 9 provide box plots for the worst estimation and stabilization examples. Fig. 10 and 11 provide the box plots for the mean accuracies. Neither the three axis determination nor the stabilization was successful at orbit inclinations lower than 30 deg. This is due to the well-known fact that the geomagnetic field is almost a constant vector. There is no torque in that direction and stabilization is not possible. Moreover, the three-axis motion is not observable in case of almost constant geomagnetic field vector. The three-axis stabilization is possible for the orbits with inclinations starting with about 40 degrees. The minimal mean and maximal stabilization and estimation errors are at about 60 degrees. The errors increase slightly for the near polar orbits. The geomagnetic induction vector lies almost in the orbital plane with very small out of plane component. As a result, the torque is generally available both in plane and out of plane. However, with only two magnetorquers the variability in the control torque construction is limited which leads to the degraded accuracy.

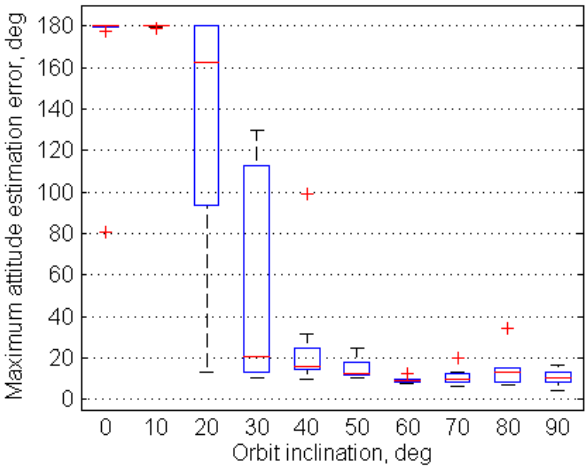

Fig. 8. The worst accuracy for the attitude estimation depending on the orbit inclination

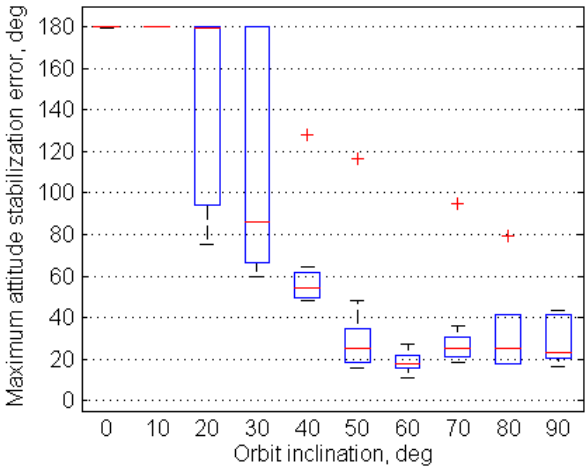

Fig. 9. The worst stabilization accuracy depending on the orbit inclination

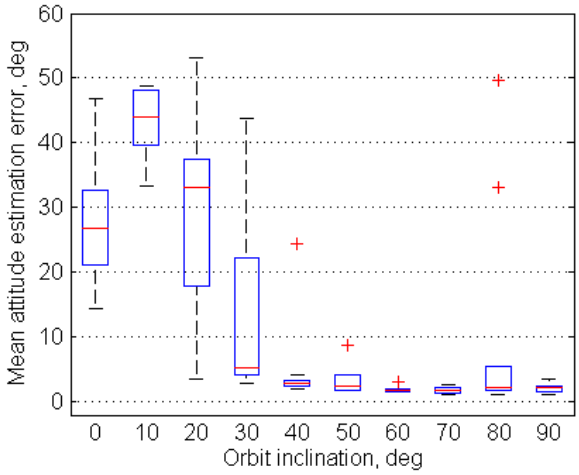

Fig. 10. Mean attitude estimation accuracy depending on the orbit inclination

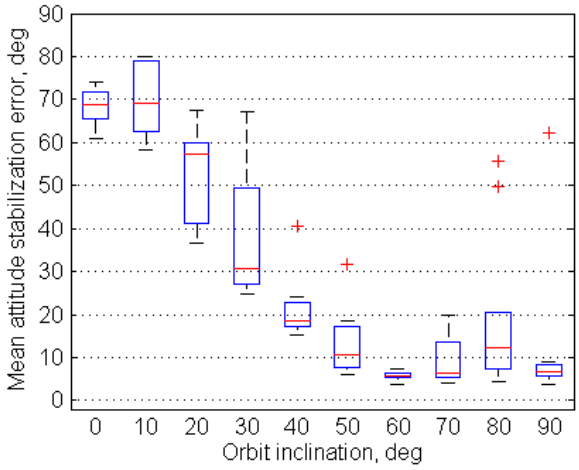

Fig. 11. Mean attitude stabilization accuracy depending on the orbit inclination

Consider how the estimation and stabilization accuracies depend on the orbit altitude. The orbit inclination is assumed to be 51.7 deg. All the parameters of the numerical simulation are the same as for in the previous example. For each orbit altitude a set of numerical experiments is performed. Fig. 12 and 13 present box plots of the mean attitude estimation and attitude stabilization accuracy depending on the orbit altitude. Since the measurement errors are fixed at value σ_{meas}=50 μV and the geomagnetic field decreases with increasing orbit altitude, then the signal-to-noise ratio worsens. Starting from altitude of 4000 km the EKF does not converge, the errors of estimation are too large and as a result the three-axis stabilization does not achieved. Nevertheless, the two magnetorquers are still able to stabilize the satellite for orbits up to 3500 km of altitude. However, the mean estimation errors as well as mean stabilization accuracy are steadily increasing with altitude.

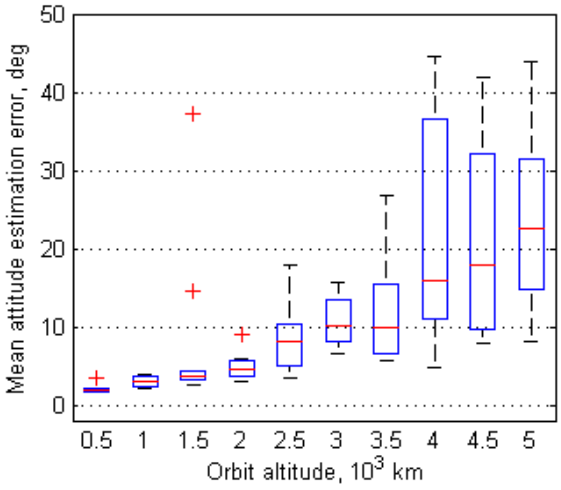

Fig. 12. Mean attitude estimation accuracy depending on the orbit altitude

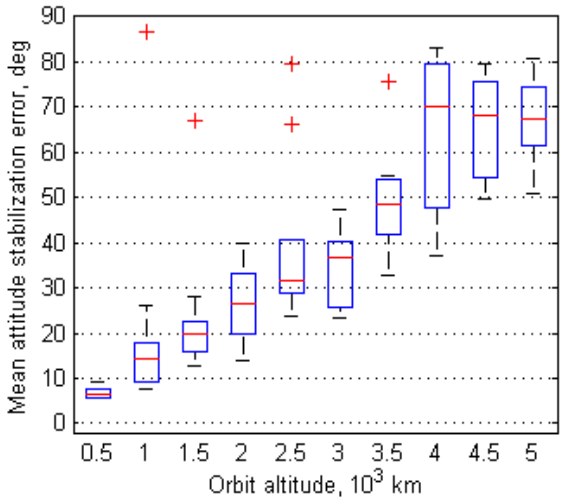

Fig. 13. Mean attitude stabilization accuracy depending on the orbit altitude

VII. Conclusion

Satellite three-axis attitude estimation and stabilization algorithms using two magnetorquers are proposed. Attitude estimation and stabilization accuracy with the Lyapunov control depends on the orbit inclination. The best performance is observed for the moderately inclined and very low earth orbits. The stabilization error is about 20 deg while the estimation error is 10 deg in the worst case. This relatively low accuracy may suffice some CubeSat missions or act as a backup measure.

Acknowledgment

The work supported by the Russian Science Foundation, grant № 17-71-20117.

References

[1] J. C. Springmann, A. J. Sloboda, A. T. Klesh, M. W. Bennett, and J. W. Cutler, “The attitude determination system of the RAX satellite,” *Acta Astronaut.*, vol. 75, pp. 120–135, Jun. 2012.

[2] O. Khurshid, J. Selkäinaho, H. E. Soken, E. Kallio, and A. Visala, “Small satellite attitude determination during plasma brake

deorbiting experiment," *Acta Astronaut.*, vol. 129, pp. 52–58, Dec. 2016.
[3] J. D. Searcy and H. J. Pernicka, "Magnetometer-Only Attitude Determination Using Novel Two-Step Kalman Filter Approach," *J. Guid. Control. Dyn.*, vol. 35, no. 6, pp. 1693–1701, Nov. 2012.
[4] M. L. Psiaki, F. Martel, and P. K. Pal, "Three-axis attitude determination via Kalman filtering of magnetometer data," *J. Guid. Control. Dyn.*, vol. 13, no. 3, pp. 506–514, May 1990.
[5] H. E. Söken, "An Attitude Filtering and Magnetometer Calibration Approach for Nanosatellites," *Int. J. Aeronaut. Sp. Sci.*, vol. 19, no. 1, pp. 164–171, Mar. 2018.
[6] E. J. Lefferts, F. L. Markley, and M. D. Shuster, "Kalman Filtering for Spacecraft Attitude Estimation," *J. Guid. Control. Dyn.*, vol. 5, no. 5, pp. 417–429, 1982.
[7] M. E. Pittelkau, "Kalman Filtering for Spacecraft System Alignment Calibration Introduction," *J. Guid. Control. Dyn.*, vol. 24, no. 6, pp. 1187–1195, 2001.
[8] E. Gai, K. Daly, J. Harrisdn, and L. Lemos, "Star-Sensor-Based Satellite Attitude / Attitude Rate Estimator," *J. Guid. Control Dyn.*, vol. 8, no. 5, pp. 560–565, 1985.
[9] K. Xiong, T. Liang, and L. Yongjun, "Multiple model Kalman filter for attitude determination of precision pointing spacecraft," *Acta Astronaut.*, vol. 68, no. 7–8, pp. 843–852, Apr. 2011.
[10] M. Abdelrahman and S.-Y. Park, "Integrated attitude determination and control system via magnetic measurements and actuation," *Acta Astronaut.*, vol. 69, no. 3–4, pp. 168–185, Aug. 2011.
[11] D. S. Ivanov, M. Y. Ovchinnikov, V. I. Penkov, D. S. Roldugin, D. M. Doronin, and A. V. Ovchinnikov, "Advanced numerical study of the three-axis magnetic attitude control and determination with uncertainties," *Acta Astronaut.*, vol. 132, pp. 103–110, 2017.
[12] D. Ivanov, M. Ovchinnikov, and D. Roldugin, "Three-Axis Attitude Determination Using Magnetorquers," *J. Guid. Control. Dyn.*, vol. 41, no. 11, pp. 2455–2462, Nov. 2018.
[13] M. Y. Ovchinnikov, V. I. Penkov, D. S. Roldugin, and A. V. Pichuzhkina, "Geomagnetic field models for satellite angular motion studies," *Acta Astronaut.*, vol. 144, pp. 171–180, Mar. 2018.
[14] A. A. Tikhonov and K. G. Petrov, "Multipole models of the earth's magnetic field," *Cosm. Res.*, vol. 40, no. 3, pp. 203–212, 2002.
[15] "Delfi-n3Xt Attitude Determination and Control Subsystem." [Online]. Available: http://www.delfispace.nl/delfi-n3xt/attitude-determination-and-control-subsystem. [Accessed: 20-May-2017].
[16] D. S. Ivanov, M. Y. Ovchinnikov, and V. I. Penkov, "Laboratory study of magnetic properties of hysteresis rods for attitude control systems of minisatellites," *J. Comput. Syst. Sci. Int.*, vol. 52, no. 1, 2013.
[17] "Analog-to-Digital Converter Design Guide High-Performance, Stand-Alone A/D Converters for a Variety of Embedded Systems Applications." [Online]. Available: http://www.t-es-t.hu/download/microchip/ds21841c.pdf. [Accessed: 21-May-2017].
[18] R. E. Kalman and R. S. Bucy, "New Results in Linear Filtering and Prediction Theory," *Trans. ASME, Ser. D, J. Basic Eng.*, vol. 83, pp. 95–108, 1961.
[19] J. R. Wertz, *Spacecraft Attitude Determination and Control*. Dordrecht/Boston, London: Acad. press, 1990.
[20] M. Y. Ovchinnikov, D. S. Roldugin, D. S. Ivanov, and V. I. Penkov, "Choosing control parameters for three axis magnetic stabilization in orbital frame," *Acta Astronaut.*, vol. 116, pp. 74–77, Nov. 2015.
[21] M. Y. Ovchinnikov, D. S. Roldugin, and V. I. Penkov, "Three-axis active magnetic attitude control asymptotical study," *Acta Astronaut.*, vol. 110, pp. 279–286, Nov. 2015.
[22] F. Celani, "Robust three-axis attitude stabilization for inertial pointing spacecraft using magnetorquers," *Acta Astronaut.*, vol. 107, pp. 87–96, Nov. 2015.
[23] I. G. Malkin, *Some problems in the theory of nonlinear oscillations*. Oak Ridge: U.S. Atomic Energy Commission, Technical Information Service, 1959.
[24] J. Li, M. Post, T. Wright, and R. Lee, "Design of Attitude Control Systems for CubeSat-Class Nanosatellite," *J. Control Sci. Eng.*, vol. 2013, pp. 1–15, 2013.